Available online at www.sciencedirect.com
ScienceDirect
Polymer 48 (2007) 2434–2443
polymer
www.elsevier.com/locate/polymer

Morphology change of asymmetric diblock copolymer micellar films during solvent annealing

Xue Li [a,*], Juan Peng [c], Yan Wen [a], Dong Ha Kim [b,c,**], Wolfgang Knoll [c]

[a] School of Chemistry and Chemical Engineering, University of Jinan, 106 Jiwei Road, Jinan, Shandong 250022, People's Republic of China
[b] Division of Nano Sciences and Department of Chemistry, Ewha Womans University, 11-1 Daehyun-Dong, Seodaemun-Gu, Seoul 120-750, South Korea
[c] Max Planck Institute for Polymer Research, Ackermannweg 10, 55128 Mainz, Germany

Received 28 August 2006; received in revised form 16 January 2007; accepted 7 February 2007
Available online 25 February 2007

Abstract

The morphology change of an asymmetric polystyrene-*block*-poly(2-vinyl pyridine) (PS-*b*-PVP) diblock copolymer micellar film was investigated during solvent vapor annealing in chloroform. Initially, smaller islands in nanometer-length scale form at the film surface. Further annealing results in the growth of the islands composed of the PS-*b*-PVP cylinders above the bottom brush layer. For comparison, a film of the block copolymer prepared from THF solution (without micellar structure) was also studied. The surface morphology of the film from THF evolves via spinodal dewetting mechanism during solvent vapor annealing. At a long time solvent vapor annealing, the two kinds of the films display the same surface morphologies, which are determined by the interplay between the surface field and autodewetting.
© 2007 Elsevier Ltd. All rights reserved.

Keywords: Asymmetric diblock copolymer; Solvent annealing; Morphology change

1. Introduction

Block copolymers (BCP) can self-assemble into a range of well-defined, ordered nanostructures including spheres, cylinders, lamellae, and double gyroids, depending on the relative volume fraction of the constituent polymers [1–4]. Thin films of block copolymers are recognized as ideal candidates for use as templates and scaffolds for the engineering of nanostructures with applications ranging from magnetic storage to optoelectronic materials, etching resists and sensors. Recently, it has been demonstrated that solvent annealing can be utilized as one important approach to produce a long-range ordered thin film of a block copolymer [5–15]. For example, Niu and Saraf described a dynamical feature in highly ordered block copolymer films made by solvent annealing and discussed about the mechanism [5]. Fukunaga et al. investigated the effect of the solvent removal speed on the resulting morphologies of ABC triblock copolymer films during solvent annealing and reported that large-scale alignment of the microdomains was obtained [8]. Xuan et al. obtained well-ordered hexagonally packed nanocylinders in the symmetric diblock copolymer poly(styrene-*block*-methyl methacrylate) (PS-*b*-PMMA) thin films by controlling the selectivity of the solvent, film thickness and the vapor exposure times [9]. Peng et al. systematically studied the effect of solvent selectivity on the solvent-annealed block copolymer thin films. Different film structures are formed in symmetric PS-*b*-PMMA thin films after solvent annealing depending on the nature of the solvent [11,12]. Cong et al. showed that water (it is not a solvent for PS and P4VP) can induce the morphology change of polystyrene-*block*-poly(4-vinylpyridine) (PS-*b*-P4VP) micellar thin films [13]. Zhao et al. investigated the surface morphologies of thin asymmetric PS-*b*-P4VP films after

* Corresponding author.
** Corresponding author. Division of Nano Sciences and Department of Chemistry, Ewha Womans University, 11-1 Daehyun-Dong, Seodaemun-Gu, Seoul 120-750, South Korea.
E-mail addresses: lixue0312@yahoo.com (X. Li), dhkim@ewha.ac.kr (D.H. Kim).

0032-3861/$ - see front matter © 2007 Elsevier Ltd. All rights reserved.
doi:10.1016/j.polymer.2007.02.054

annealing in methanol vapor, a selective solvent for minority P4VP block [14]. Kim et al. showed that solvent evaporation at a controlled rate could provide a very simple but robust route to generate almost defect-free microstructures over large areas in poly(styrene-*block*-ethylene oxide) (PS-*b*-PEO) diblock copolymer films [10]. Most of the approaches mentioned above are focused on the relative orientation of a microphase-separated morphology with respect to a substrate surface when the experimental variables, such as the surface field, film thickness, solvent evaporation rate, solvent selectivity, annealing conditions, etc. are changed [5–15]. However, the detailed mechanisms involved in these treatments remain unclear. Moreover, correlation between the initial morphologies of block copolymer thin films prepared from different solvents and the resulting morphological developments are little considered.

Generally, preferential wetting of one block at an interface occurs to minimize the free energy of the system, leading to a parallel orientation of the microdomains [16–18]. In symmetric diblock copolymers, quantization of the film thickness often takes place. When the thickness of the film is not commensurate to the equilibrium lamellar spacing, either holes or islands are nucleated on the film surface to adjust the local film thickness to the preferred quantized values. When the interaction with the surface is significantly reduced, a thickness incommensurability may lead to perpendicular orientation of the lamellae with respect to the boundary surfaces [17].

However, when the interaction between one block and the substrate surface (the surface field) is very strong, a stable brush can form. In the case of dense brush, the homopolymer or the same blocks cannot penetrate into the brush deeply, which may lead to autodewetting of the materials. It has been reported that PS homopolymer dewets PS brush layer attached to the substrate surface under certain conditions [19]. Large disordered droplets of block copolymers also autophobically dewet the dense brush layer of the ordered copolymer chains in block copolymer thin films slightly above the order–disorder transition temperature [20,21]. Lee et al. reported that autophobic dewetting played an important role in the formation of the hierarchical surface pattern induced by residual solvent in thin films of the PS-*b*-PVP block copolymer ($\varphi_{PS} = 0.37$) [22].

It has been reported that various kinds of block copolymer micelles could be prepared in solution [23,24]. In particular, nanometer-sized micellar monolayer films prepared from block copolymer micelle solutions using Langmuir–Blodgett self-assembly, dip coating or spin-coating methods are versatile as templates for nanostructured materials, where the stability of the morphology is critical in future applications [25–33]. In this work, we studied the time evolution of the surface structures of the micellar films of an asymmetric diblock copolymer of PS-*b*-PVP during solvent annealing. For comparison, another type of the block copolymer film prepared from THF solution without micellar structure was also studied. With this approach, a systematic investigation into the effects of the initial morphology on the development of surface structures in thin block copolymer films after solvent annealing was performed.

2. Experimental part

2.1. Materials

Polystyrene-*block*-poly(2-vinyl pyridine) (PS-*b*-PVP) with a polydispersity index of 1.07 was purchased from Polymer Source, Inc. The number average molecular weights of PS and PVP blocks were 54,900 g/mol and 18,600 g/mol, respectively.

2.2. Substrate preparation

Silicon (Si) substrates (~2.5 cm × 2.5 cm) with a native silicon oxide layer on the surface were cleaned with a mixed solution of concentrated H_2SO_4 and H_2O_2 (30%) (70/30 v/v) at 80 °C for 30 min, thoroughly rinsed with Milli-Q water and dried under a stream of nitrogen gas.

2.3. Film preparation

The micellar films were prepared by spin coating the 0.5 wt% and 0.25 wt% toluene solutions of PS-*b*-PVP on silicon substrates at 2500 rpm. The films were dried at 50 °C in a vacuum for 12 h to remove residual solvent. The film thicknesses measured by using a Tencor-10 surface profiler on silicon substrates were about 22 nm and 11 nm, respectively. To change the initial morphology of a block copolymer film, a ~22 nm thick film was also prepared from tetrahydrofuran (THF) solution of PS-*b*-PVP. Since THF is a nonselective solvent for PS and PVP, the as-cast thin film prepared from THF solution shows no micellar structure. The films prepared from different solvents were exposed to the saturated chloroform vapor in a closed desiccator at room temperature for different periods of time, and then the samples were removed to ambient atmosphere and promptly dried.

2.4. Characterization

Atomic Force Microscopic (AFM) images were obtained using a Digital Instruments Dimension 3100 scanning force microscope in the tapping mode using Olympus cantilevers with spring constants ranging between 33.2 N/m and 65.7 N/m and resonant frequencies of 277.3–346.3 Hz (as specified by the manufacturer).

X-ray Photoelectron Spectroscopy (XPS) was performed on an ESCALAB 250 (Thermo Electron Co., America) spectrometer with an Al Kα ($h\nu = 1486.6$ eV) mono X-ray source. Spectra were obtained at a take-off angle of 15°.

3. Results and discussion

3.1. The morphology change of PS-b-PVP micellar films under chloroform vapor

3.1.1. PS-b-PVP micellar films with ~22 nm thickness

It is well known that in a selective solvent for the PS blocks, e.g., toluene, nanometer-sized micelles consisting of

a soluble PS corona and an insoluble PVP core are formed above the critical micelle concentration. A micellar film of diblock copolymers can be easily formed by spin coating. The AFM height image and phase contrast image of a spin-cast PS-*b*-PVP micellar film from 0.5 wt% toluene solution on a silicon substrate surface are shown in Fig. 1. The brighter and darker areas in the images correspond to the PVP microdomains and the PS matrix, respectively. The surface exhibits a closely packed quasi-hexagonal structure, which is consistent with the surface morphology observed in Refs. [26,32,33].

After the film was treated in the chloroform vapor for different times, the surface of the film was examined with AFM. At relatively short annealing time in chloroform vapor, small islands of about 40 nm in diameter appear on the film surface with an average height of the islands being only ~4 nm (Fig. 2a). At a higher magnification, the surface does not exhibit any lateral structures, indicating that the micellar structure disappears at this moment. This morphology may represent a disordered, intermediate stage driven by the interplay between microphase separation and dewetting. If the film is treated further, the islands grow to form larger domains. The microphase separation is driven by long-range repulsion due to incompatibility between the two component blocks, whereas dewetting is by destabilizing long-range intermolecular forces such as dispersive or van der Waals' forces. In the current case, the morphology evolution is influenced by the combination of the two simultaneous processes, both of which lead to the decrease of the free energy of the system. The size and the height of the islands increase with annealing time as evidenced in Fig. 2b and c. The brighter parts are composed of islands and the lower or darker regions are defined as the bottom layer. The line scans in Fig. 2a–c also show the height of the islands (the height from the top surfaces of islands to the bottom layer surface). To distinguish the structure difference between the top surfaces of islands and the bottom layer surface, AFM images were taken from the island surface and the bottom layer surface. Fig. 2b1 and b1′ are the AFM height and phase images obtained from the selected island surfaces (black box b1 in Fig. 2b), respectively, after annealing for 13 h. Fig. 2c1 and c1′ are the AFM height and phase images obtained from the selected island surfaces (black box c1 in Fig. 2c), respectively, after annealing for 24 h. One can always find a striped surface pattern at an island surface (Fig. 2b1 and c1). The composition of the copolymer used in this work ($\varphi_{PVP} = 0.25$) and the surface free energies of PS and PVP ($\gamma_{PS} = 39.8$ mN/m, $\gamma_{PVP} = 45.1$ mN/m [34]) suggest that the copolymers in islands form cylinder morphology with a PVP core and a PS shell. Although the heights of the islands increase with annealing time, the striped surface patterns remain unchanged. The lateral period between neighboring cylinders determined by AFM is about 50 nm. This value is larger than the height of the islands (Fig. 3). However, in the lower regions in Fig. 2b and c, the surfaces are very smooth and featureless. Fig. 2c2 and c2′ show the AFM height and phase images taken at the lower regions from the selected black box c2 in Fig. 2c. This can be attributed to the formation of a brush layer of PS-*b*-PVP on silicon surface. The film thickness in the lower regions is ~11 nm from the AFM measurement of the scratched surface. The changes of the island height and the thickness of the bottom layer (the height from the surface of darker regions to reference silicon substrate surface) with time were measured and displayed in Fig. 3. It should be noted that at relatively short annealing times (1–13 h), the data points showing the higher thickness of bottom layer are not the thickness of brush layer. It may contain excess block copolymers, which may be in disordered state. If the annealing time exceeds 24 h, the thickness of the bottom layer almost does not change. It can be deduced that this value (~11 nm) is the thickness of the bottom brush layer.

In order to investigate the origin of the stripped patterns, a film was annealed for 4 h and then the surface morphology was carefully monitored by AFM. When the image was

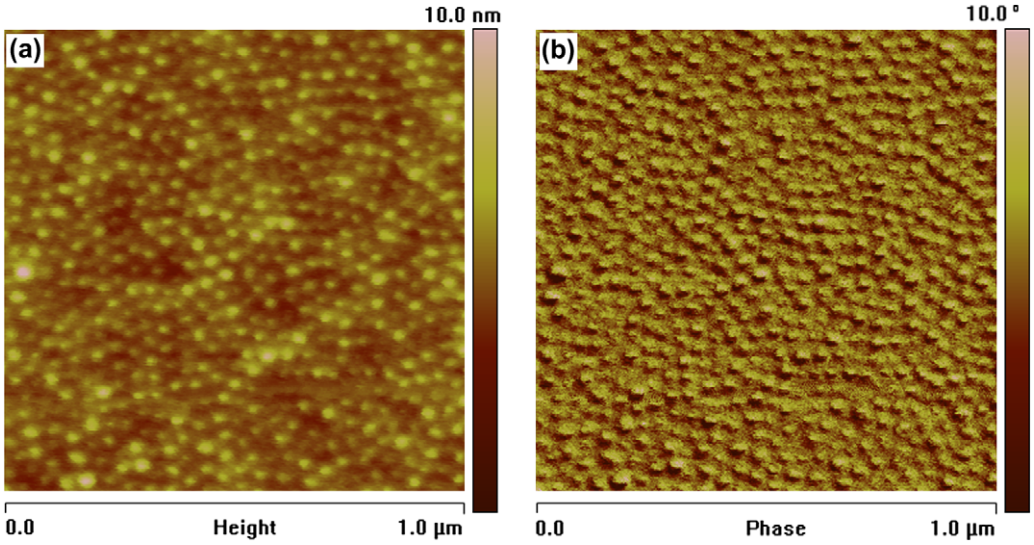

Fig. 1. AFM height and phase images of the micellar film of the PS-*b*-PVP block copolymer spin cast on silicon substrates from 0.5 wt% toluene solution.

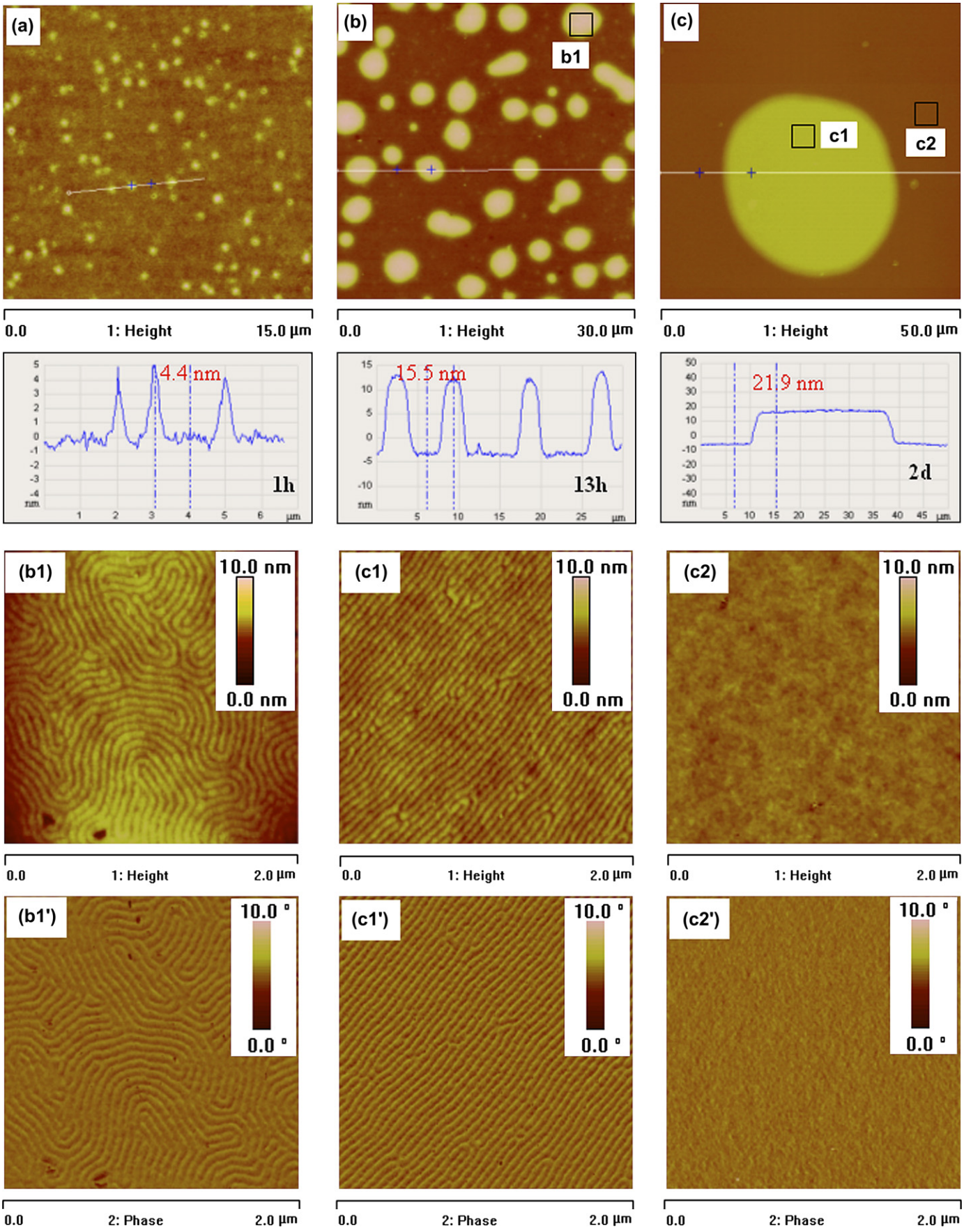

Fig. 2. AFM height images and their sectional profiles along the lines shown in the images of the micellar films of the PS-*b*-PVP block copolymer after solvent annealing in chloroform vapor for (a) 1 h, (b) 13 h, and (c) 24 h. (b1), (c1) and (c2) are the AFM height images scanned from the selected areas marked as black boxes b1, c1 and c2 in (b) and (c), respectively. (b1′), (c1′) and (c2′) are the AFM phase images from the selected areas marked as black boxes b1, c1 and c2 in (b) and (c), respectively.

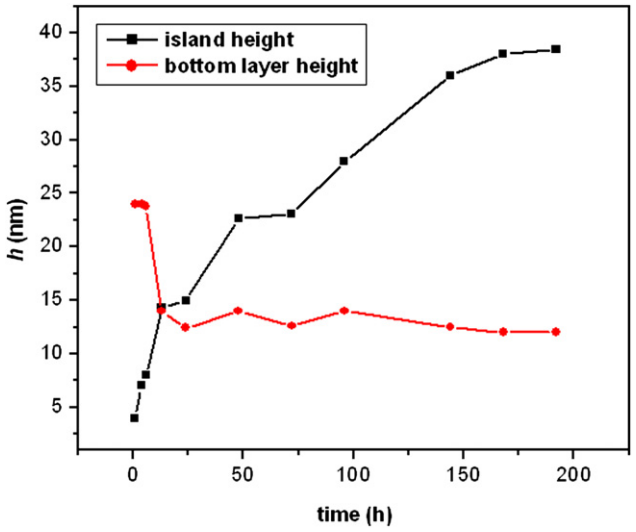

Fig. 3. Changes of the island height and the bottom layer height as a function of solvent vapor annealing time.

scanned at a lower magnification, small islands were also observed. Fig. 4a displays that the sizes of islands (about 200–900 nm in diameter and about 7 nm in height) at the film surface are larger than those in Fig. 2a. Fig. 4c shows the morphology obtained at a higher magnification which appears at the surface of what may be considered the initial stage of cylinder formation. This morphology may be interpreted as the initiation of aggregate formation of the copolymer chains above the brush layer to form cylinders. Then more amounts of block copolymer chains migrate to the nucleation sites, leading to the growth of the cylinders/islands (the diameter and the length of the cylinders increase with time). The observed islands in Fig. 2b and c are composed of cylinders. With increasing the annealing time, the smaller islands merge into larger ones. The island growth should follow the 2D Ostwald ripening mechanism [35–37]. However, only islands of less than 50 nm height on the film surface were observed since the initial thickness of the micellar film was in the order of ~22 nm.

3.1.2. PS-b-PVP micellar films with ~11 nm thickness

It is well known that PS-*b*-PVP forms a stable brush layer adjacent to the substrate due to the strong interaction of PVP block to the SiO_x substrate in a thin film [22]. In order to monitor the structural evolution of a bottom brush layer at substrate surface upon annealing, a film of ~11 nm (prepared from a 0.25% toluene solution) was treated in chloroform vapor for different times. Fig. 5 shows the AFM images of the block copolymer film before and after annealing. For the spin-cast film, the spherical surface domains similar to the ones in Fig. 1a were observed. However, the domain sizes are smaller than those in Fig. 1a. After treatment with chloroform vapor, the film surface becomes smooth and featureless and the morphology does not change with annealing time, indicating that no excess block copolymer chains exist to form cylinders/islands at the film surface after the formation of the brush layer. The contact angle is close to that of pure PS film (~90°) and any N1s peaks were not observed in high-resolution XPS spectrum (Fig. 6), providing evidence that the surface of the brush layer is composed of PS blocks. Since the block copolymer chains in the bottom brush layer are tightly attached to the substrate surface, the brush layer is quite stable. Santer and Rühe observed that the topography of the brushes of poly(methyl methacrylate-*block*-glycidyl-methacrylate) (PMMA-*b*-PGMA) diblock copolymer can be turned into a flat, featureless surface after exposing the samples to a good solvent for both blocks, though the as-prepared brushes can appear as ripple-like, worm-like and spherical-like morphologies [38,39].

It has been reported that PS-*b*-PVP chains adsorbed from the copolymer solution onto mica surface form a homogeneous brush with PVP blocks anchored on the polar mica surface which corresponds to a lamellar coating. The thickness (e) of the PVP layer and the equilibrium average brush height (L) of PS segments can be expressed by [40]:

$$e = kN_A^{11/23}N_B^{-6/23} \quad (1)$$

$$L = a_{PS}N_B^{21/23}N_A^{-4/23} \quad (2)$$

where k is the prefactor (~1.1), N_A and N_B are the numbers of repeat unit of PVP and PS, respectively, and a is the monomer length ($a_{PS} = 0.19$ nm). The calculation yields a PVP thickness (e) value of 0.25 nm and PS height (L) value of 9.82 nm. Thus the total thickness of the brush is about 10.07 nm in solution.

Generally, the thickness value measured by AFM in thin films of block copolymers is smaller than the calculated value in solution because PS will take a collapsed conformation after solvent extraction. However, in this case, the bottom brush layer has a height of ~11 nm based on the AFM image of the scratched surface (Fig. 3), which is in good agreement with the predicted value calculated from Eqs. (1) and (2). This means that the chain packing in the upper PS brush layer is more pronounced than that at the bottom PVP brush layer since PS block has larger molecular weight than PVP block. Therefore, it can be deduced that a dense PS layer forms at the top surface of the silicon substrate. It has been reported that, in the case of the dense brush layer, the homopolymer or the same blocks cannot penetrate into the brush deeply, leading to autodewetting of the materials [41].

3.1.3. The morphology change mechanism of a micellar film with ~22 nm thickness

It has been reported that PEO, PVP (hydrophilic polymers) and PMMA (hydrophobic polymer) have a relatively strong interaction with SiO_x or mica substrate surfaces [9,42,43]. When PS-*b*-PMMA or PS-*b*-PEO is cast on a Si substrate with a SiO_x surface layer, the PMMA or PEO preferentially segregates to the substrate while the PS segregates to the air interface due to the presence of asymmetric boundary condition. However, in a selective solvent for PMMA or PEO, solvent vapor molecules have a stronger tendency to attract PMMA or PEO

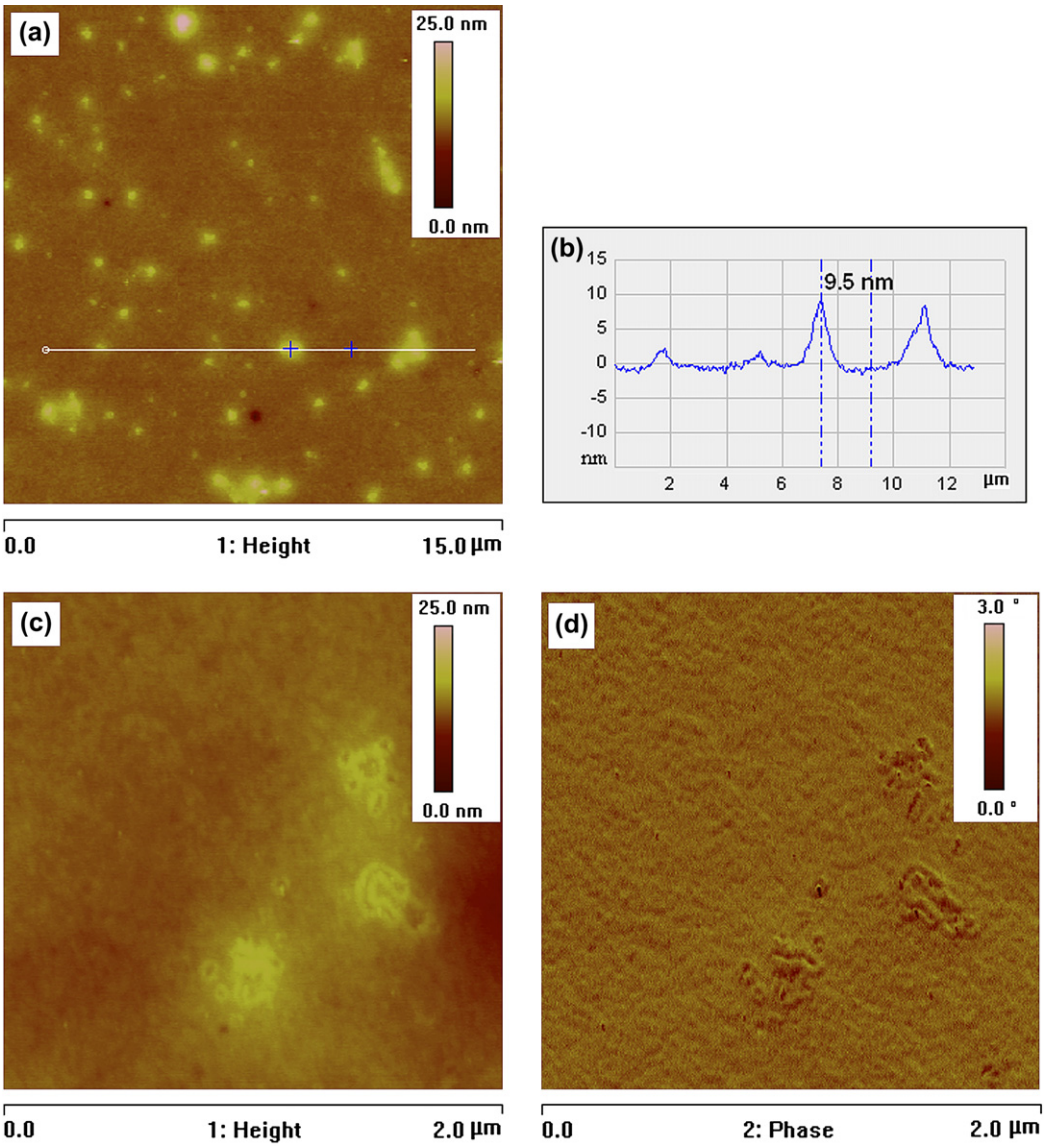

Fig. 4. AFM images of the micellar films of the PS-*b*-PVP block copolymer after solvent annealing in chloroform vapor for 4 h. (a) is AFM height image obtained at a lower magnification and (b) is its sectional profile along the line in the image. (c) and (d) are AFM height and phase images scanned at a higher magnification to show the initial stage of cylinder formation or nucleation sites of islands.

than PS to maximize the PMMA–solvent or PEO–solvent contacts. Xuan et al. observed that PMMA blocks are pulled toward the film surface under selective solvent vapor environments. Using solvent annealing method, thin PS-*b*-PMMA or PS-*b*-PEO copolymer films exhibiting surface-parallel or surface-perpendicular morphology or one with well-ordered hexagonally packed cylinders could be obtained [9,10].

However, for thin PS-*b*-PVP diblock copolymer films, the VP blocks strongly anchor to the SiO_x surface via the interaction between pyridine units and OH groups at the substrate surface [44]. Upon solvent vapor annealing with a good solvent for PVP block, a stable brush layer on SiO_x surface forms. Therefore the morphology changes are different from those of PS-*b*-PMMA or PS-*b*-PEO films.

The mechanism of the morphology change of a ~22 nm thick micellar film during solvent annealing can be explained as follows. Chloroform is known as a good solvent for both PS and PVP with a slight selectivity toward P2VP [45]. In the presence of chloroform solvent, the swollen PVP core and the PS matrix in the film (Fig. 7a) become more mobile and can reorganize themselves easily (Fig. 7b). More PVP blocks in micellar cores migrate to the SiO_x surface. The main driving force is the strong polar interaction of substrate surface with VP units. This process leads to the formation of a bottom brush layer (Fig. 7c and d), where the PS blocks adopt a stretched conformation due to the composition asymmetry of the block copolymer. At the same time, parts of the PS-*b*-PVP molecules migrate to the film surface and begin to self-assemble into cylinders (with a PVP core and a PS shell) oriented parallel to the substrate surface. Then the cylinders grow to form islands upon increasing the annealing time (Fig. 7d). In the case of the dense brush layer (Fig. 7f), if

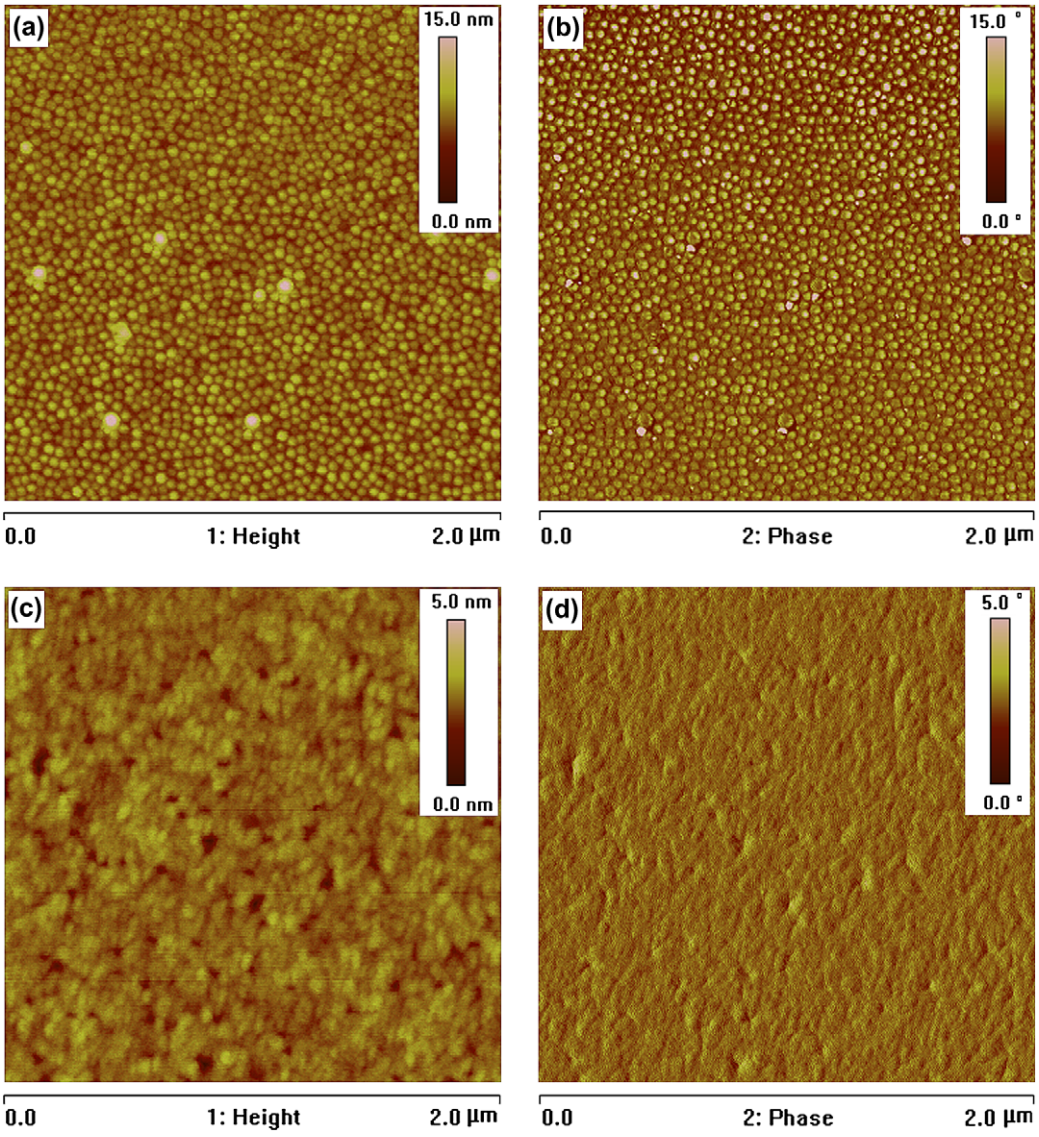

Fig. 5. (a) and (b) are AFM height and phase images of the micellar films of the PS-*b*-PVP block copolymer spin cast on silicon substrates from 0.25 wt% toluene solution. (c) and (d) show AFM height and phase images of the micellar films after solvent vapor annealing for 5 days.

the PS blocks above the brush layer cannot penetrate into the brush deeply, an interface with corresponding interfacial free energy will be established [41]. The excess energy associated with this interface can induce dewetting (autodewetting). It has been reported that PS homopolymer can dewet PS brush layer attached to the substrate surface under certain conditions [19]. Large disordered droplets of block copolymers also autophobically dewet the dense brush layer of the ordered copolymer chains in block copolymer thin films slightly above the order–disorder transition temperature [20,21]. In our case, autophobic dewetting between the dense brush layer and the PS-*b*-PVP cylinders (with a PVP core and a PS shell) above it dominates the island growth process at longer annealing time. Therefore, the lamellar morphology cannot form on the brush layer. Elbs et al. observed that for films of the asymmetric diblock copolymer PS_{14}-*b*-PVP_{86} with small thickness, a stepped surface and a striped surface morphology were observed after vapor treatment in chloroform. In the first terrace of polystyrene-*block*-poly(2-vinyl pyridine)-*block*-poly(*tert*-butyl methacrylate) (PS_{17}-*b*-PVP_{26}-*b*-$PBMA_{57}$) triblock copolymer film, the striped pattern was also observed [46].

3.2. The morphology change of PS-b-PVP films prepared from THF upon annealing in chloroform vapor

If the initial films of the PS-*b*-PVP block copolymers were prepared from different solvents, e.g., THF (almost nonselective to PS and PVP), one may find that the morphology development process in chloroform vapor is different from that of the film spin cast from toluene solutions. Fig. 8 shows the morphologies of a ~22 nm thick film prepared from THF and treated in chloroform vapor for 0 h, 4 h, 1 day and 4 days. The AFM height and phase images of the spin-cast film display that the cylinders of PVP with parallel orientation and perpendicular orientation coexist (Fig. 8a and b). Upon annealing in chloroform vapor, the film forms a bicontinuous

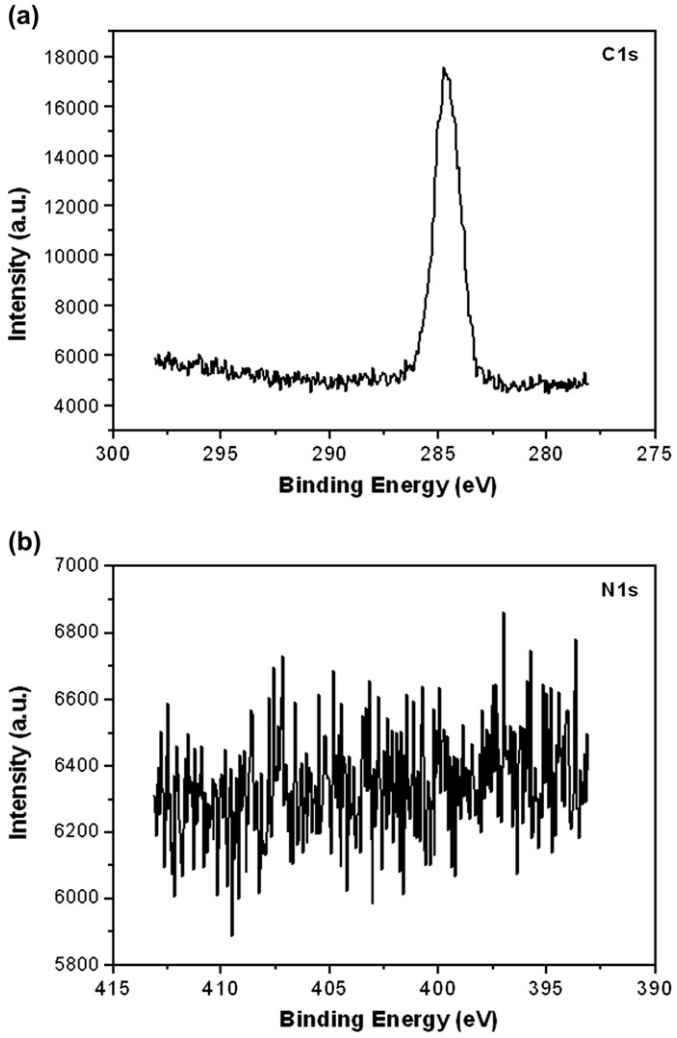

Fig. 6. High-resolution XPS C1s and N1s spectra of ~11 nm thick micellar films of the PS-*b*-PVP block copolymer after solvent vapor annealing for 5 days.

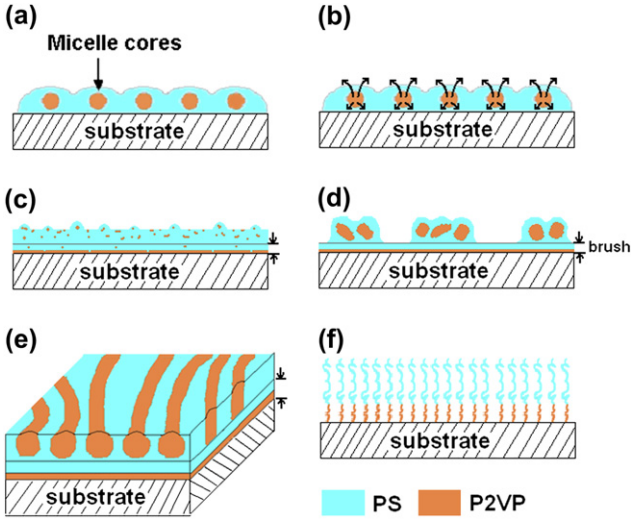

Fig. 7. Schematic illustration of time evolution of the microstructure in PS-*b*-PVP micellar film with ~22 nm thickness. (a) As-cast PS-*b*-PVP micellar film; (b) swollen PVP chains begin to migrate to both SiO_x and film surfaces, when exposed to chloroform vapor for a certain period of time; (c) a brush layer on SiO_x surface begins to form, and at the same time PS-*b*-PVP chains self-assemble to form small islands/cylinders on film surface; (d) islands are formed on the film surface after a long time annealing; (e) plane view of a island surface in (d); (f) schematic illustration of the substrate surface induced PS-*b*-PVP diblock copolymer brush. The figures were not drawn to scale.

spinodal-like pattern on the bottom brush layer. The pattern eventually evolves into droplets, as shown in Fig. 8a–e. It has been reported that thin symmetric PS-*b*-PMMA diblock copolymer films can form bicontinuous pattern on a "brush" of height of $L/2$ (L is the interlamellar spacing in the bulk) on the substrate after annealing at temperatures higher than the bulk order–disorder transition temperature [20]. However, all the surfaces of the terraces in Fig. 8c–e form a stripped morphology. The phase image in Fig. 8f shows both the brush and the terrace regions. Comparing Fig. 2 with Fig. 8, one can find that, for the two kinds of films prepared from toluene and THF, though their initial morphologies are different, the same patterns are obtained after chloroform vapor treatment for a long time scale. However, the evolution processes to the final structures are different from each other. THF is a nonselective solvent for both PS and PVP blocks. When PS-*b*-PVP is cast from THF solution on a silicon substrate with a native SiO_x surface layer, the PVP blocks preferentially segregate to the substrate surface and form a brush layer. The other block copolymer chains adsorbed on the brush layer cannot evolve into their equilibrium states due to the fast evaporation of solvent during spin coating. That is, the bottom brush layer has already been formed during the spin-coating process. When the film is annealed in chloroform vapor, the solvent molecules can penetrate into the PVP and the PS microdomains uniformly and lead to the film rupture spontaneously (known as spinodal dewetting). The film rupturing process is driven by surface energy [20,47], and the hills will grow at expense of the valleys. After annealing for a long time, the spinodal-like pattern decays into large droplets. The dewetting process is accompanied by the evolution of the nonequilibrium cylindrical microdomains being annealed to equilibrated ones.

4. Conclusion

Upon solvent vapor annealing in chloroform, the effect of the initial morphology at the free surface of an asymmetric PS-*b*-PVP diblock copolymer on the topographical structures of the resulting films was investigated where the PVP component has a strong preferential affinity for the SiO_x substrate. For a micellar film of the block copolymer prepared from toluene solution, the surface morphology develops via a nucleation and growth mechanism, while it evolves via spinodal dewetting mechanism for a film prepared from THF solution. Identical final morphologies are obtained for the two kinds of the films after a long time solvent vapor annealing. These results reveal that the initial morphology can influence the process of the pattern evolution that develops at the free

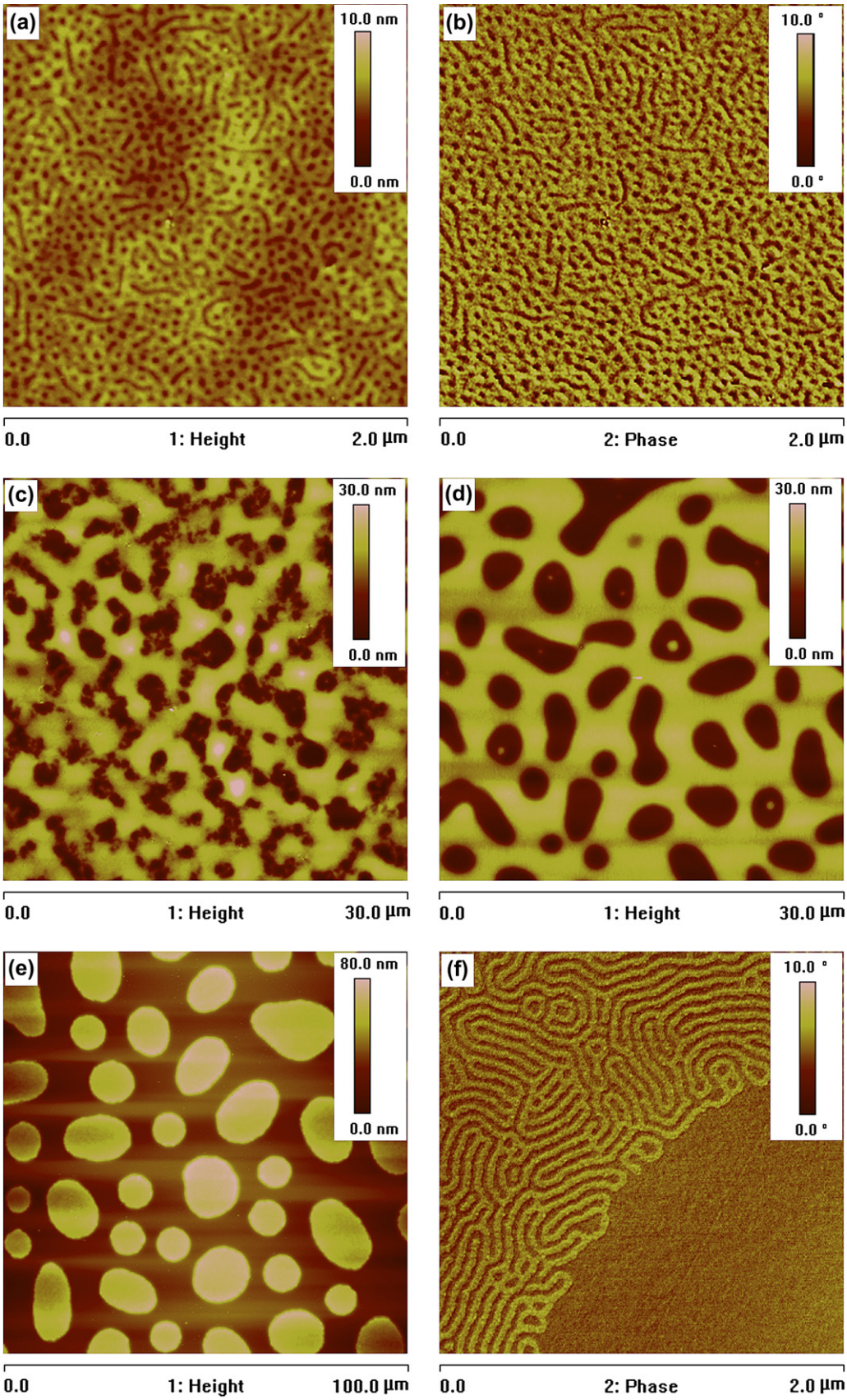

Fig. 8. (a) and (b) are the AFM height and phase images of the spin-cast PS-*b*-PVP film obtained from THF solution. (c)–(e) are the AFM height images of the films after solvent annealing in chloroform vapor for 4 h, 1 day, and 4 days, respectively. (f) is the AFM phase image from sample (d) showing the difference between the island surface and the bottom brush layer surface.

surface of the PS-*b*-PVP diblock copolymer during solvent vapor annealing.

Acknowledgements

This work was funded by the National Natural Science Foundation of China (20674030), Shandong Natural Science Foundation (2006ZRB01092) and the Doctorial Foundation of University of Jinan, PR China (B0541). Financial support in part from Deutsche Forschungsgemeinschaft (DFG) within the Schwerpunktprogramm 1165 (SPP 1165: KN 224/15-1) and Max Planck Gesellschaft (MPG) is acknowledged. This work was supported by Seoul Research and Business Development Program (10816).

References

[1] Hamley IW. The physics of block copolymers. New York: Oxford University Press; 1998.
[2] Fredrickson GH, Bates FS. Annu Rev Mater Sci 1996;26:501–50.
[3] Hashimoto T, Shibayama M, Fujimura M, Kawai H. In: Meier DJ, editor. Block copolymers, science and technology. London: Harwood Academic; 1983. p. 63–108.
[4] Fasolka MJ, Mayes AM. Annu Rev Mater Res 2001;31:323–55.
[5] Niu S, Saraf RF. Macromolecules 2003;36:2428–40.
[6] Kim G, Libera M. Macromolecules 1998;31:2569–77.
[7] Alexandridis P, Spontak RJ. Curr Opin Colloid Interface Sci 1999;4:130–9.
[8] Fukunaga K, Elbs H, Magerle R, Krausch G. Macromolecules 2000; 33:947–53.
[9] Xuan Y, Peng J, Cui L, Wang H, Li B, Han Y. Macromolecules 2004; 37:7301–7.
[10] Kim SH, Misner MJ, Russell TP. Adv Mater 2004;16:2119–23.
[11] Peng J, Kim DH, Knoll W, Xuan Y, Li BY, Han YC. J Chem Phys 2006;125:064702.
[12] Peng J, Xuan Y, Wang HF, Li BY, Han YC. Polymer 2005;46:5767–72.
[13] Cong Y, Zhang ZX, Fu J, Li J, Han YC. Polymer 2005;46:5377–84.
[14] Zhao JC, Jiang SC, Ji XL, An LJ, Jiang BZ. Polymer 2005;46:6513–21.
[15] Han X, Liu H, Dong Y, Hu Y. Chin J Chem Eng 2005;13:498–503.
[16] Coulon G, Deline VR, Russell TP, Green PF. Macromolecules 1989; 22:2581–9.
[17] Anastasiadis SH, Russell TP, Satija SK, Majkrzak CF. Phys Rev Lett 1989;62:1852–5.
[18] Huang E, Pruzinsky S, Russell TP. Macromolecules 1999;32:5299–303.
[19] Maas JH, Cohen Stuart MA, Leermakers FAM, Besseling NAM. Langmuir 2000;16:3478–81.
[20] Limary R, Green PF. Macromolecules 1999;32:8167–72.
[21] Hamley IW, Hiscutt EL, Yang YW, Booth C. J Colloid Interface Sci 1999;209:255–60.
[22] Lee SH, Kang H, Kim YS, Char K. Macromolecules 2003;36:4907–15.
[23] Shen HW, Eisenberg A. J Phys Chem B 1999;103:9473–87.
[24] Bhargava P, Zheng JX, Li P, Quirk RP, Harris FW, Cheng SZD. Macromolecules 2006;39:4880–8.
[25] Kästle G, Boyen H-G, Weigl F, Lengl G, Herzog T, Ziemann P, et al. Adv Funct Mater 2003;13:853–61.
[26] Spatz JP, Mösser S, Hartmann C, Möller M, Herzog T, Krieger M, et al. Langmuir 2000;16:407–15.
[27] Sohn B-H, Yoo S-I, Seo B-W, Yun S-H, Park S-M. J Am Chem Soc 2001;123:12734–5.
[28] Yun S-H, Sohn B-H, Jung JC, Zin W-C, Lee J-K, Song O. Langmuir 2005;21:6548–52.
[29] Hwang W, Ham MH, Sohn B-H, Huh J, Kang YS, Jeong W, et al. Nanotechnology 2005;16:2897–902.
[30] Weng C-C, Hsu K-F, Wei K-H. Chem Mater 2004;16:4080–6.
[31] Chan Y, Mi Y. Polymer 2004;45:3473–80.
[32] Li X, Lau KHA, Kim DH, Knoll W. Langmuir 2005;21:5212–7.
[33] Li X, Tian SJ, Ping Y, Kim DH, Knoll W. Langmuir 2005;21:9393–7.
[34] Sauer BB, Dee GT. Macromolecules 2002;35:7024–30.
[35] Bassereau P, Brodbreck D, Russell TP, Brown HR, Shull KR. Phys Rev Lett 1993;71:1716–9.
[36] Ardell AJ. Phys Rev Lett 1995;74:4960.
[37] Bassereau P, Brodbreck D, Russell TP, Brown HR, Shull KR. Phys Rev Lett 1995;74:4961.
[38] Santer S, Rühe J. Polymer 2004;45:8279–97.
[39] Kizhakkedathu JN, Kumar KR, Goodman D, Brooks DE. Polymer 2004;45:7471–89.
[40] Bossé F, Schreiber HP, Eisenberg A. Macromolecules 1993;26:6447–54.
[41] Liu Y, Rafailovich MH, Sokolov J, Schwarz SA, Zhong X, Eisenberg A, et al. Phys Rev Lett 1994;73:440–3.
[42] Huang Y, Liu X-B, Zhang H-L, Zhu D-S, Sun Y-J, Yan S-K, et al. Polymer 2006;47:1217–25.
[43] Li X, Han YC, An LJ. Polymer 2003;44:8155–65.
[44] Spatz JP, Möller M, Noeske M, Behm RJ, Pietralla M. Macromolecules 1997;30:3874–80.
[45] Elbs H, Krausch G. Polymer 2004;45:7935–42.
[46] Elbs H, Drummer C, Abetz V, Krausch G. Macromolecules 2002;35: 5570–7.
[47] Rixens B, Severac R, Boutevin B, Lacroix-Desmazes P. Polymer 2005; 46:3579–87.